MicroRNA-23a-3p inhibitor decreases osteonecrosis incidence in a rat model

YULEI DONG[1], TAO LI[2], YULONG LI[1], SHAODA REN[3], JUNFEN FAN[3] and XISHENG WENG[1]

[1]Department of Orthopedic Surgery, Peking Union Medical College Hospital, Peking Union Medical College, Chinese Academy of Medical Science, Beijing 100730; [2]Department of Orthopedic Surgery, The Affiliated Hospital of Qingdao University, Qingdao, Shandong 266003; [3]Center of Tissue Engineering, Chinese Academy of Medical Sciences and Peking Union Medical College, Institute of Basic Medical Sciences and School of Basic Medicine, Beijing 100005, P.R. China

Received September 20, 2016; Accepted June 6, 2017

DOI: 10.3892/mmr.2017.7808

Abstract. The mechanism of steroid-associated femoral head necrosis remains unclear. The present study investigated the role of microRNA-23a-3p (miR-23a-3p) in the incidence of osteonecrosis in a rat model. An miR-23a-3p mimic, an inhibitor and a negative control were transfected into bone mesenchymal stem cells using a lentiviral vector, and then injected into the steroid-induced femoral head necrosis model. Osteonecrosis incidence was assessed by micro computed tomography and histopathology. Low-density lipoprotein receptor-related protein 5 (LRP-5) expression was assessed by immunohistochemistry. The results demonstrated the incidence of osteonecrosis decreased in the miR-23a-3p inhibitor group compared with the miR-23a-3p mimic group (18.2% vs. 75%; P<0.05). The ratio of bone volume/total volume and trabecular thickness were significantly increased in the miR-23a-3p inhibitor group compared with the miR-23a mimic group. The expression level of LRP-5 was higher in the miR-23a-3p inhibitor group. The present study indicated that miR may provide a novel and alternative approach for understanding the mechanism underlying steroid-associated necrosis of the femoral head.

Introduction

Steroid-associated osteonecrosis is common as steroids are a widely-used treatment for a number of diseases. Steroid-associated osteonecrosis leads to high disability rates as it results in partial or complete loss of the ability to walk. However, there remains no ideal treatment for steroid-associated femoral head necrosis, the mechanisms of which remain to be elucidated.

Certain researchers have described abnormalities in the number or in the function of bone progenitor cells in osteonecrosis (1,2). The current hypothesis is that osteonecrosis could be associated with an imbalance between osteoblast formation and necrosis (3,4). In addition, osteogenic differentiation of mesenchymal stem cells is attenuated by glucocorticoids (5,6). MicroRNAs (miRs) are small molecular regulators of gene expression and serve critical roles in stem cell differentiation (7,8). The authors previously screened and compared miR expression between patients with steroid-associated femoral head necrosis and normal adults (9). miR-23a-3p was the most significantly upregulated miR in patients with femoral head necrosis. The authors also previously demonstrated that miR-23a-3p was significantly downregulated during osteogenic differentiation (10). Overexpression of miR-23a-3p inhibited osteogenic differentiation of bone mesenchymal stem cells (BMSCs), whereas downregulation of miR-23a-3p enhanced the process (10). The authors also previously confirmed that low-density lipoprotein-receptor-related protein 5 (LRP-5) is a direct target of miR-23a-3p (10). Therefore it is hypothesized is that inhibiting miR-23a-3p may decrease the incidence of osteonecrosis. In the present study, the effect of miR-23a-3p in a rat model of osteonecrosis was investigated.

Materials and methods

Animals. The Animal Experimentation Ethics Committee of Peking Union Medical College Hospital approved the present study protocol. Sprague-Dawley male adult rats of between 4 and 12 weeks old were obtained from Charles River Laboratories (Wilmington, MA, USA). BMSCs were isolated from the lower limbs of 4-week old rats. A total of 18, 12-week old rats (400-450 g) were reared in pairs in custom-designed plexiglass cages (50x35x20 cm) under standard laboratory conditions (12-h light/dark cycle; 24-25˚C; humidity, 50-55%) with free access to food and water during the study.

Isolation and culture of the BMSCs. Primary rat BMSCs were harvested by flushing the bone marrow cavity of the femurs

Correspondence to: Dr Xisheng Weng, Department of Orthopedic Surgery, Peking Union Medical College Hospital, Peking Union Medical College, Chinese Academy of Medical Science, 9 Dongdan 3rd Alley, Beijing 100730, P.R. China
E-mail: xshweng@medmail.com.cn

Key words: bone mesenchymal stem cells, femoral head necrosis, osteonecrosis, animal model, microRNA

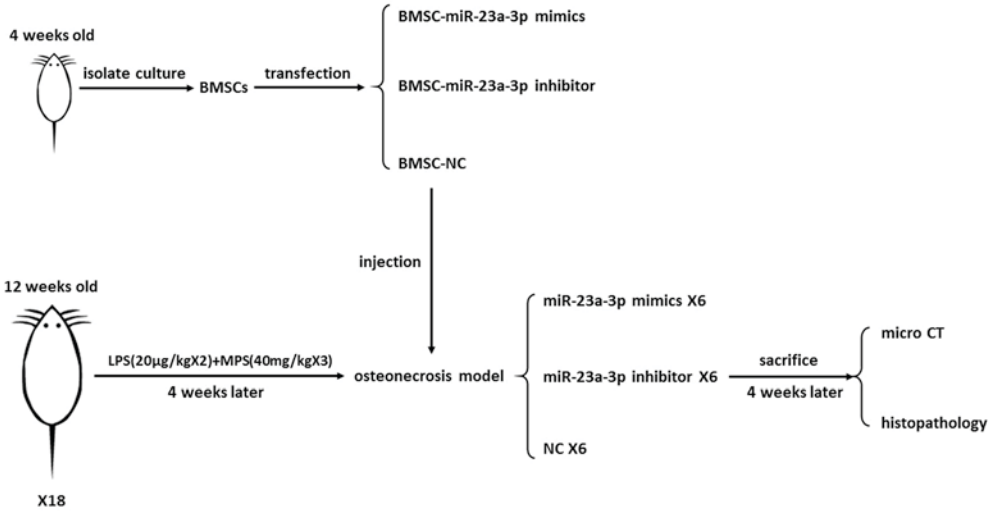

Figure 1. Flow diagram of the study. LPS, low-dose lipopolysaccharide; MPS, methylprednisolone; rBMSC, rat bone mesenchymal stem cell; CT computed tomography; NC, negative control; miR, microRNA.

and tibias of 4-week-old rats with Dulbecco's modified Eagle's medium (DMEM; Gibco; Thermo Fisher Scientific, Inc., Waltham, MA, USA). The cell suspension was plated and cultured in DMEM supplemented with 10% fetal bovine serum (Gibco; Thermo Fisher Scientific, Inc.), 100 U/ml penicillin and 100 U/ml streptomycin at 37˚C in a humidified 5% CO_2 incubator. The culture medium was replaced and non-adherent cells were removed every 3-4 days. The cells were treated with trypsin and were passaged by a ratio of ~1:3 at sub-confluence. The cells from the third passage were transfected with a lentiviral vector and used in the following experiments.

Animal model establishment. In the present study, the steroid-induced osteonecrosis model was established in rats by two injections of low-dose (20 μg/kg) lipopolysaccharide (LPS) combined with three subsequent injections of high-dose methylprednisolone (40 mg/kg). The 12-week-old rats were administered intraperitoneal injections of 20 μg/kg LPS (*Escherichia coli* 055:B5; Merck KGaA, Darmstadt, Germany) twice with an interval of 24 h. The rats received three times of intramuscular injection of 40 mg/kg methylprednisolone sodium succinate (Pfizer, Inc., New York, NY, USA) on day 3, 4 and 5 at an interval of 24 h (11). The order in which the experiment was performed is illustrated in Fig. 1.

Transfection of miR-23a-3p in rat BMSCs (rBMSCs). Synthetic miR-23a-3p mimic (sequence: 5'-ATCACATTGCCAGGGATTTCC-3'), miR-23a-3p inhibitor (sequence: 5'-GGAAATCCCTGGCAATGTGAT-3') and negative control (NC, sequence: 5'-TTCTCCGAACGTGTCACGTTTC-3') were purchased from GenePharma (Sunnyvale, CA, USA) along with lentiviral green fluorescent protein (GFP)-tagged vector LV3-pGLV-h1-GFP-puro. The synthetic mRNA ($1x10^9$ transducing units/ml) was transfected into BMSCs according to the manufacturer's protocol. The most effective multiplicity of infection (MOI) was decided according to the pilot experiment (data not shown). rBMSCs were plated onto 10 cm dishes at a density of $1x10^6$ cells/dish in 5 ml media and transfected using a GFP-tagged lentiviral vector (lenti-23a-mimic-GFP, lenti-23a-inhibitor-GFP and lenti-GFP) at an MOI of 100 plaque-forming unit/cell in the presence of 5 μl polybrene (Merck KGaA). Fresh media was added at 24 h following transfection. Transfection efficiency was analyzed by calculating the number of GFP tagged cells out of the total number of cells after 72-96 h following transfection. The BMSCs was imaged under a fluorescence microscope (x200). Transfection rate was measured by flow cytometry (9) (Fig. 2). The BMSCs of the rats were isolated and cultured under standard conditions. The transfection rate was >95%.

Local injection of rBMSCs. The rBMSCs which stably expressed lenti-23a-mimic-GFP, lenti-23a-inhibitor-GFP or the lenti-GFP control were harvested. The cells were treated with 2.5% trypsin and resuspended in PBS. A total of 0.2 ml PBS containing $1x10^6$ cells were prepared from the marrow cavity of the femur of each animal. The injection technique was practiced in a preliminary experiment (data not shown). The rats were anesthetized by chloral hydrate (Pharmacy, Peking Union Medical College Hospital, Peking, China). The midline approach to the knee was taken. The skin of the knee was incised and a needle-mounted syringe was inserted superior to the patellar and parallel to the shaft of the femur. Once the initial resistance was overcome, the needle was firmly attached, and could be inferred to be in the femoral marrow cavity. The cell suspension was injected locally into the bone marrow cavity from the mid-point of femoral condyles, 4 weeks following the establishment of the animal model.

Micro computed tomography (CT) scan and quantitative analysis. A total of 4 weeks following the localized injection of rBMSCs, the rats were sacrificed and the midline of the femoral condyles was sampled and fixed in 10% buffered neutral formalin solution until examination. The samples were scanned by Inveon micro CT manufactured by Siemens AG (Munich, Germany) at a voltage of 60 kV and a current of 400 μA, with entire scan length of 20 mm in a spatial resolution of 10 μm. The images were reconstructed using Inveon analysis workstation (version 2.0; Siemens AG). The key features for femoral head necrosis diagnosis using micro CT

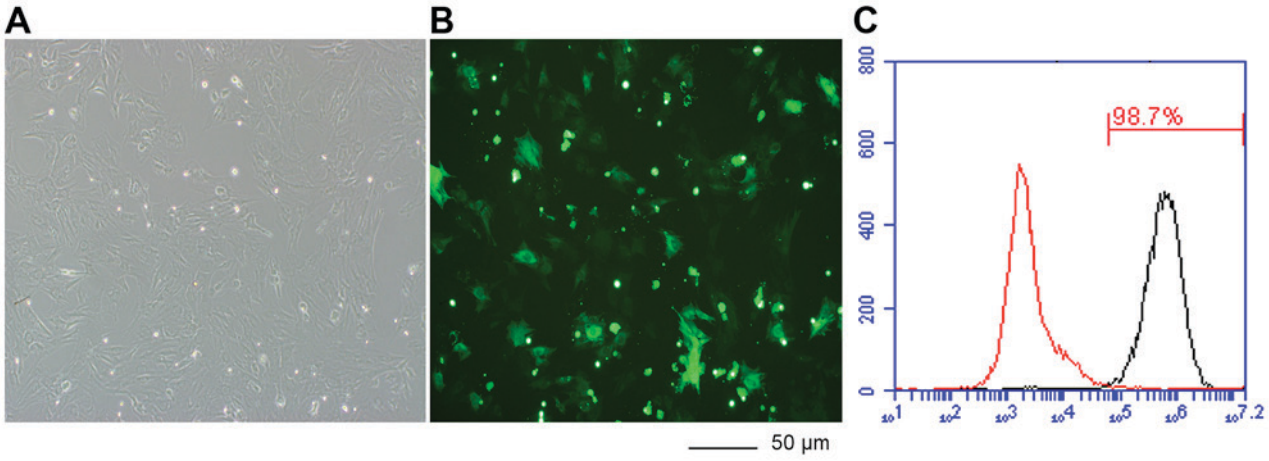

Figure 2. Images of rat bone mesenchymal stem cells following transfection (A) was under light microscopy and (B) under fluorescent microscopy) and (C) the results of the flow cytometry.

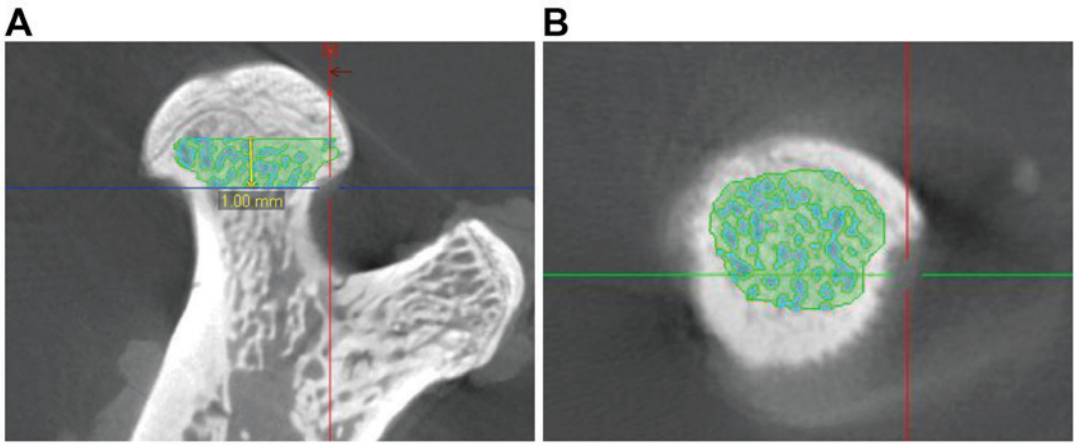

Figure 3. Region of interest selected on the (A) sagittal and (B) transverse sections of the head of the femur and highlighted in green.

were fracture of the trabeculae, cystic degeneration, sclerotic banding or flattening of the femoral head. A total of two independent researchers performed concordant blind diagnosis. Out of 50 transverse sections taken, 1 mm below the center of the epiphyseal line was selected as the region of interest (ROI) for the analysis and comparison of trabecula parameters (Fig. 3). On the cross-section, the cortical bone and cancellous bone were separated manually by auto trace. Then, the trabeculae and bone marrow were separated by the threshold function. The threshold function could separate the bone marrow and trabecular bone by adjusting the Min and Max CT Unit-Hounsfield Unit (HU) to select the bone marrow and trabecular bone separately according to their different HU. Subsequently, the bone volume/total volume (BV/TV), bone surface area/bone volume (BS/BV), trabecular thickness (Tb.Th), trabecular number (Tb.N) and trabecular spacing (Tb.Sp) in the ROI were calculated respectively by the workstation.

Histopathology. The femur specimens were fixed in 10% buffered neutral formalin solution for 72 h at room temperature and followed by decalcification with 10% EDTA-0.1 M phosphate buffer (pH 7.4). Following decalcification, the tissues were dehydrated in graded ethanol, embedded in paraffin, cut into 4-μm-thick sections in the coronal plane. Subsequently the specimens were processed with a routine hematoxylin and eosin stain at room temperature with hematoxylin stain for 5-20 min and the eosin for 30 sec, prior to being evaluated for the degree of osteonecrosis present. All sections were assessed blind by two independent authors using a light microscope (Leica Microsystems GmbH, Wetzlar, Germany). The diagnosis of osteonecrosis was established based on the presence of empty lacunae or pyknotic nuclei of osteocytes in the bone trabeculae, accompanied by surrounding bone marrow cell necrosis (12). If the diagnosis differed between the two examiners, a third opinion was sought.

Immunohistochemistry. Immunohistochemistry for LRP-5 was performed. The 4-μm-thick sections were deparaffinization with xylene at room temperature, and rehydrated with graded alcohol, treated to aid antigen retrieval and incubated with the primary antibody (1:300; Goat anti-LRP5; Everest Biotech Ltd., Bicester, UK; cat. no. EB06771) at 4˚C overnight. Subsequently, the biotinylated secondary antibody (rabbit anti-goat; Abcam, Cambridge, UK; cat. no. ab6741; 1:1,000) were applied at room temperature for 1 h and 3,3'-diaminobenzidine tetrahydrochloride substrate was used to stain the

sections. The sections were then treated with hematoxylin and mounted. All sections were photographed using a light microscope (Leica Microsystems GmbH) on the same setting. Each section was imaged three times. Image-Pro Plus (version 6.0; Media Cybernetics, Inc., PA, USA) was used to measure the mean density of each photo.

Statistical analysis. The Student's t-test or Fisher's exact test was performed to compare the variables between the two groups. Two-way analysis of variance was performed to compare the variables more than two groups. The least significant difference method was applied. The parameters were expressed as the mean ± standard deviation. Statistical analysis was performed using SPSS for Windows (version 17.0; SPSS Inc., Chicago, IL, USA). $P<0.05$ was considered to indicate a statistically significant difference.

Results

Micro CT scan of femoral head. In the present study three rats (two in the miR-23a-3p mimic group and one in the NC group) succumbed to the high dose of corticosteroid injection. A single femur sample was damaged in the miR-23a-3p inhibitor group. The rest of the rats were alive for the duration of the experiment. Therefore, in the final analysis, 8, 11 and 10 samples were included in the mimic, inhibitor and NC groups, respectively. The femoral head of the miR-23a-3p inhibitor group exhibited a rounded shape and condense trabeculae without significant cystic degeneration. By contrast, the femoral head of the mi-23a-3p mimic group exhibited scattered trabeculae and cystic degeneration (Fig. 4A).

Quantitative analysis of the trabeculae parameters. The quantitative analysis demonstrated that the BV/TV and Tb.Th were significantly increased in the miR-23a-3p inhibitor group compared with the miR-23a-3p mimic group. The Tb.Sp was significantly decreased in the miR-23a-3p inhibitor group compared with the miR-23a-3p mimic group (Fig. 4B).

Histopathology. The prevalence of osteonecrosis were 18.2% (2/11) and 75% (6/8) in miR-23a-3p-inhibitor and miR-23a-3p-mimic groups, respectively ($P<0.05$, mimic vs. inhibitor). The average number of empty bone lacunae was significantly less in the miR-23a-3p inhibitor group. The mean density of immunohistochemical images of LRP-5 positive cell was significantly higher in the miR-23a-3p inhibitor group (Fig. 4B and C).

Discussion

A number of bone diseases, including osteoporosis and femoral head necrosis may develop if the balance of BMSC differentiation is disrupted. Understanding the mechanism of osteogenic differentiation of BMSCs is crucial to getting an improved insight in the pathogenesis of skeletal disorders and to increase treatment options. Increasing evidence has indicated that miRs serve a vital role in the osteogenic differentiation of BMSCs.

miR-23a, located on chromosome 19p13.12, has been widely researched in recent years. It has been reported that miR-23a expression is upregulated in multiple types of cancer, including hepatocellular carcinoma (13), lung cancer (14) and colorectal cancer (15), indicating that miR-23a participates in the carcinogenesis and metastasis of cancer. In addition, miR-23a has been proved to promote myelination in the central nervous system (16). A recent study revealed that miR-23a exhibited a significantly higher expression level in the bone tissue of osteoporotic patients compared with controls (17).

The authors previously identified that miR-23a was involved in the osteogenesis of BMSCs. Inhibiting miR-23a enhanced the osteogenic differentiation of BMSCs (10). In the present study, it was demonstrated that the injection of a miR-23a-3p inhibitor could decrease the incidence of osteonecrosis in a rat model. The authors previously demonstrated that miR-23a was partially complementary to a site in the 3' untranslated region of LRP-5 (10). LRP-5 expression was increased during the osteogenesis of BMSCs, while miR-23a-3p expression was reduced. Furthermore, miR-23a-3p overexpression resulted in downregulation of LRP-5, whereas functional inhibition of miR-23a-3p upregulated LRP-5, suggesting that LRP-5 was regulated by miR-23a during osteogenic differentiation. Immunohistochemical staining also demonstrated increased intensity of LRP-5 staining in the miR-23a-3p inhibitor group compared with the NC and miR-23a-3p mimic group, which was consistent with the previous cell experiment. LRP-5 is a single-pass transmembrane protein belonging to the LRP family. LRP-5 is closely associated with homologue LRP-6, which is another co-receptor for the canonical Wnt signaling pathway. LRP-5 serves a crucial role in bone formation. Mice lacking LRP-5 exhibit a decrease in bone mass, while LRP-5 activation increases bone mass (18). LRP-5 variants were proved to be associated with low peak bone mass and osteoporosis, which may control bone formation by inhibiting serotonin synthesis in the duodenum (19).

Increasing evidence indicates that miR serves a vital role in the development of various bone diseases. However, the biological role of miR in the pathogenesis of non-traumatic osteonecrosis of femoral head (ONFH) remains to be completely investigated. Wu *et al* (20) used miR microarray chip analysis, and revealed that 22 miRs were upregulated and 17 miRNAs were downregulated in the non-traumatic ONFH samples compared with the femoral neck fracture samples. Wang *et al* (21) also described abnormal expression of miR in the serum of patients with ONFH. Yamasaki *et al* (22) demonstrated that that mature miR-210 was expressed around the necrotic area. In addition, von Willebrand factor and vascular endothelial growth factor were also highly expressed in the miR-210 expressing cells. Jia *et al* (23) further studied the level of mature miR-17-5p and demonstrated that it was significantly decreased in non-traumatic osteonecrotic samples compared with the osteoarthritis samples. miR-17-5p modulated osteoblastic differentiation and cell proliferation by targeting Mothers against decapentaplegic homolog 7 in non-traumatic osteonecrosis (23). To the best of the authors' knowledge, the present study was the first study to investigate the role of miR in femoral head necrosis in an animal model. miR may provide a novel and alternative approach for understanding the mechanism underlying steroid-associated necrosis of the femoral head.

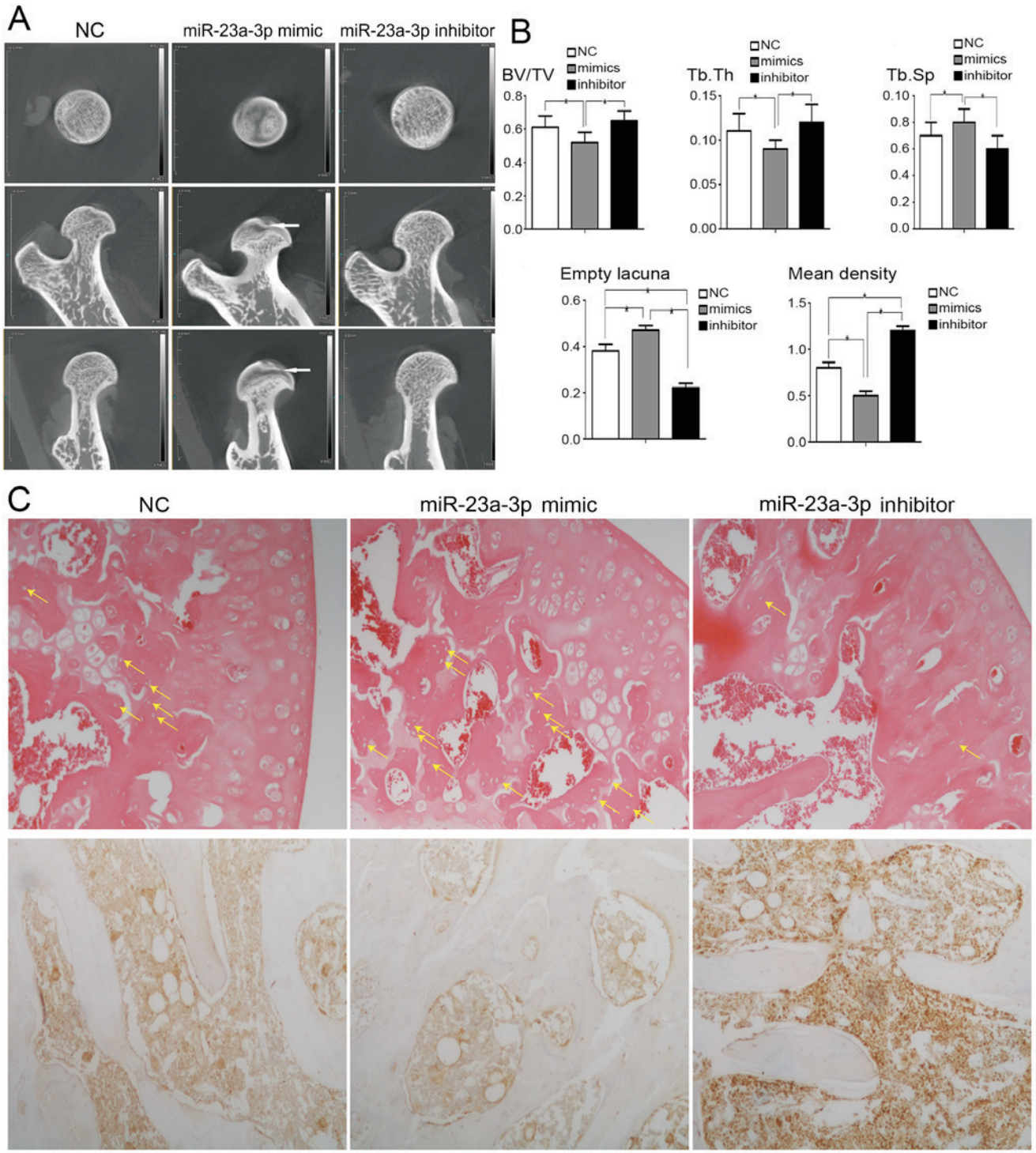

Figure 4. Quantitative analysis of alterations in femoral parameters associated with bone thickness and density. (A) Representative micro computed tomography images of the proximal femur. miR-23a-3p-inhibitor: The shape of the femoral head was round with condensed trabeculae. miR-23a-3p-mimic: The femoral head was flattened and the trabeculae were scattered with cystic degeneration (white arrow). (B) Bar graphs demonstrating that BV/TV and Tb.Th were lower in the miR-23a-3p mimic group, and Tb.Sp was higher in the miR-23a-3p mimic group. The incidence of empty bone lacunae number was lower in the miR-23a-3p inhibitor group. The mean density of immunohistochemical images of LRP-5 positive cell was higher in the miR-23a-3p inhibitor group. *P<0.05. (C) The average number of empty bone lacuna (yellow arrow) was decreased in the miR-23a-3p inhibitor group compared with NC and miR-23a-3p mimic groups (hematoxylin and eosin stained; magnification, x100). Representative immunohistochemical images demonstrating a higher intensity of LRP-5 staining in miR-23a-3p inhibitor group compared with the NC and miR-23a-3p mimic groups (magnification, x100)., NC, negative control; BV/TV, bone volume/ total volume; Tb.Th, trabecular thickness; Tb.Sp, trabecular spacing; LRP-5, low density lipoprotein receptor-related protein-5; miR, microRNA.

In conclusion, inhibition of miR-23a caused a lower incidence of osteonecrosis, and higher expression of BV/TV and Tb.Th. miR-23a-3p may be used as a potential biomarker and therapeutic target of femoral head necrosis in the future.

Acknowledgements

The present study was supported by the National Natural Science Foundation of China (grant no. 81272009).

References

1. Hernigou P, Beaujean F and Lambotte JC: Decrease in the mesenchymal stem-cell pool in the proximal femur in corticosteroid-induced osteonecrosis. J Bone Joint Surg Br 81: 349-355, 1999.
2. Hernigou P and Beaujean F: Abnormalities in the bone marrow of the iliac crest in patients who have osteonecrosis secondary to corticosteroid therapy or alcohol abuse. J Bone Joint Surg Am 79: 1047-1053, 1997.
3. Chang JK, Ho ML, Yeh CH, Chen CH and Wang GJ: Osteogenic gene expression decreases in stromal cells of patients with osteonecrosis. Clin Orthop Relat Res 453: 286-292, 2006.
4. Lee JS, Lee JS, Roh HL, Kim CH, Jung JS and Suh KT: Alterations in the differentiation ability of mesenchymal stem cells in patients with nontraumatic osteonecrosis of the femoral head: Comparative analysis according to the risk factor. J Orthop Res 24: 604-609, 2006.
5. Cárcamo-Orive I1, Gaztelumendi A, Delgado J, Tejados N, Dorronsoro A, Fernández-Rueda J, Pennington DJ and Trigueros C: Regulation of human bone marrow stromal cell proliferation and differentiation capacity by glucocorticoid receptor and AP-1 crosstalk. J Bone Miner Res 25: 2115-2125, 2010.
6. Rauch A, Seitz S, Baschant U, Schilling AF, Illing A, Stride B, Kirilov M, Mandic V, Takacz A, Schmidt-Ullrich R, *et al*: Glucocorticoids suppress bone formation by attenuating osteoblast differentiation via the monomeric glucocorticoid receptor. Cell Metab 11:517-531, 2010.
7. Gangaraju VK and Lin H: MicroRNAs: Key regulators of stem cells. Nat Rev Mol Cell Biol 10: 116-125, 2009.
8. Lakshmipathy U and Hart RP: Concise review: MicroRNA expression in multipotent mesenchymal stromal cells. Stem Cells 26: 356-363, 2008.
9. Li T, Li H, Li T, Fan J, Zhao RC and Weng X: MicroRNA expression profile of dexamethasone-induced human bone marrow-derived mesenchymal stem cells during osteogenic differentiation. J Cell Biochem 115: 1683-1691, 2014.
10. Li T, Li H, Wang Y, Li T, Fan J, Xiao K, Zhao RC and Weng X: microRNA-23a inhibits osteogenic differentiation of human bone marrow-derived mesenchymal stem cells by targeting LRP5. Int J Biochem Cell Biol 72: 55-62, 2016.
11. Tong P, Wu C, Jin H, Mao Q, Yu N, Holz JD, Shan L, Liu H and Xiao L: Gene expression profile of steroid-induced necrosis of femoral head of rats. Calcif Tissue Int 89: 271-284, 2011.
12. Yamamoto T, Irisa T, Sugioka Y and Sueishi K: Effects of pulse methylprednisolone on bone and marrow tissues: Corticosteroid-induced osteonecrosis in rabbits. Arthritis Rheum 40: 2055-2064, 1997.
13. Bao L, Zhao J, Dai X, Wang Y, Ma R, Su Y, Cui H, Niu J, Bai S, Xiao Z, *et al*: Correlation between miR-23a and onset of hepatocellular carcinoma. Clin Res Hepatol Gastroenterol 38: 318-330, 2014.
14. Mengru C, Masahiro S, Chie S, Hideaki M, Kazuhiro K, Yuji M, Rintaro N, Akinobu Y, Li C and Akihiko G: MiR-23a regulates TGF-es TGF- Yuji M, Rintaro N, Akinobu Y, Li C and Akihiko G: MiR-23a regulates TGF-s TGF-y 38: 318-323, 2014. Oncology 41: 869-875, 2012.
15. Jahid S, Sun J, Edwards RA, Dizon D, Panarelli NC, Milsom JW, Sikandar SS, Gümüs ZH and Lipkin SM: miR-23a promotes the transition from indolent to invasive colorectal cancer. Cancer Discov 2: 540-553, 2012.
16. Lin ST, Huang Y, Zhang L, Heng MY, Ptácek LJ and Fu YH: MicroRNA-23a promotes myelination in the central nervous system. Proc Natl Acad Sci USA 110: 17468-17473, 2013.
17. Seeliger C, Karpinski K, Haug AT, Vester H, Schmitt A, Bauer JS and van Griensven M: Five freely circulating miRNAs and bone tissue miRNAs are associated with osteoporotic fractures. J Bone Miner Res 29: 1718-1728, 2014.
18. Cui Y, Niziolek PJ, MacDonald BT, Zylstra CR, Alenina N, Robinson DR, Zhong Z, Matthes S, Jacobsen CM, Conlon RA, *et al*: Lrp5 functions in bone to regulate bone mass. Nat Med 17: 684-691, 2011.
19. Yadav VK, Ryu JH, Suda N, Tanaka KF, Gingrich JA, Schütz G, Glorieux FH, Chiang CY, Zajac JD, Insogna KL, *et al*: Lrp5 controls bone formation by inhibiting serotonin synthesis in the duodenum. Cell 135: 825-837, 2008.
20. Wu X, Zhang Y, Guo X, Xu H, Xu Z, Duan D and Wang K: Identification of differentially expressed microRNAs involved in non-traumatic osteonecrosis through microRNA expression profiling. Gene 565: 22-29, 2015.
21. Wang X, Qian W, Wu Z, Bian Y and Weng X: Preliminary screening of differentially expressed circulating microRNAs in patients with steroid-induced osteonecrosis of the femoral head. Mol Med Rep 10: 3118-3124, 2014.
22. Yamasaki K, Nakasa T, Miyaki S, Yamasaki T, Yasunaga Y and Ochi M: Angiogenic microRNA-210 is present in cells surrounding osteonecrosis. J Orthop Res 30: 1263-1270, 2012.
23. Jia J, Feng X, Xu W, Yang S, Zhang Q, Liu X, Feng Y and Dai Z: MiR-17-5p modulates osteoblastic differentiation and cell proliferation by targeting SMAD7 in non-traumatic osteonecrosis. Exp Mol Med 46: e107, 2014.